Process Biochemistry 50 (2015) 221–229

Contents lists available at ScienceDirect

Process Biochemistry

journal homepage: www.elsevier.com/locate/procbio

Kinetic and equilibrium studies of adsorption of β-glucuronidase by clinoptilolite-rich minerals

Dilek Demirbüker Kavak*, Semra Ülkü

Izmir Institute of Technology, Engineering Faculty, Chemical Engineering Department, Gulbahce Koyu, 35430 Urla Izmir, Turkey

ARTICLE INFO

Article history:
Received 19 May 2014
Received in revised form 9 November 2014
Accepted 11 December 2014
Available online 27 December 2014

Keywords:
β-Glucuronidase enzyme
Clinoptilolite
Adsorption
Kinetic studies

ABSTRACT

The adsorption of the bacterial β-glucuronidase (GUS) enzyme, which is thought to be responsible for the production of reactive metabolites related to some diseases and cancer development, by clinoptilolite-rich mineral was investigated. Batch experiments were performed to analyze of the effects of the clinoptilolite amount and particle size, initial GUS concentration, shaking rate, pH and temperature on the adsorption equilibrium and kinetics. Adsorption equilibrium data were interpreted in terms of Langmuir and Freundlich isotherms; and they were well represented by the Langmuir isotherm model. The percentage of GUS removal by the clinoptilolite-rich mineral was changed in the range of 9.4–54.4% depending on its initial concentration. The kinetic data were analyzed using external film diffusion, intraparticle diffusion, pseudo-first-order and pseudo-second-order models and both external film and intraparticle diffusion appeared to be effective in GUS adsorption. Thermodynamic studies indicated that GUS adsorption is exothermic, physical and spontaneous at the temperatures investigated (288–310 K).

1. Introduction

Natural zeolites are crystalline porous aluminasilicates of group IA and IIA elements with pore and channel systems. These minerals consist of corner-sharing AlO_4 and SiO_4 tetrahedra. Their ion-exchange, adsorption, and molecular sieve properties make them unique and advantageous for use in different agricultural, chemical and environmental applications [1,2]. Recently the incorporation of organic molecules onto clinoptilolite and synthetic zeolites has attracted growing interest because their frameworks are suitable for the encapsulation and/or adsorption of different molecules. They are used for protein adsorption, separation or enzyme immobilization and have been suggested as drug support systems, antibacterial agent release matrices or bacteria loading supports [3–9]. Clinoptilolite and its modified forms were used to protect animals from feed-originating toxins by adsorbing toxic compounds in the gastrointestinal tract and preventing their passage into the circulatory system [10–14]. Purified natural clinoptilolite was reported to be harmless to the human body and recommended as an antidiarrheal drug and as antiacid agent for humans suffering from hyperacidity and showed no toxic or biological hazards [5,6,15]. Among the studies performed, those related to the use of clinoptilolite in cancer treatment, have special value; in animal models clinoptilolite treatment has improved health, prolonged life-spans and decreased tumor size [16–20]. Therefore, to identify the mechanism underlying the therapeutic effects of clinoptilolite-rich minerals, investigation of the interactions between clinoptilolite rich minerals and bioactive molecules related to health and diseases is crucial for the formulation of new materials for biomedical applications.

Considering the suggested positive role of clinoptilolite in animal health and cancer, in this study attention has been focused on an enzyme responsible for diseases. β-Glucuronidase (GUS) is an enzyme found in some mammalian and plant tissues. In the intestine, GUS activity is mostly bacterial in origin. This enzyme is responsible for drug metabolite detoxification and producing reactive metabolites related to diseases and cancer development [21–23]. Many exogenous (e.g., drugs, pesticides) as well as endogenous compounds (e.g., bilirubin, steroids, bile acids) are conjugated with glucuronic acid in the liver and excreted by the bile. The GUS enzyme catalyzes hydrolysis of glucuronides and liberates toxins and mutagens that are excreted into the gut after being glucuronated in the liver. Various carcinogens are produced by bacterial β-glucuronidase in the intestine, and the results of different studies indicate that GUS activity may be considered a cancer risk biomarker [24–27]. Food intake (such as yogurt and plants) and

* Corresponding author. Present address: Afyon Kocatepe University, Engineering Faculty, Food Engineering Department, ANS Campus, 03200 Afyonkarahisar, Turkey. Tel.: +90 0272 2281423; fax: +90 0272 2281422.
E-mail address: dkavak@aku.edu.tr (D. Demirbüker Kavak).

http://dx.doi.org/10.1016/j.procbio.2014.12.013
1359-5113/

natural bioactive compounds (such as organic acids and plant extracts) were considered for the inhibition of GUS activity in various studies [28–31].

Although there are different studies on the use of zeolites as adsorbents for biomolecules, this is the first study that investigates the adsorption of bacterial β-glucuronidase enzyme by clinoptilolite rich mineral. In this study, adsorption of the bacterial GUS (from *Escherichia coli*) on to clinoptilolite-rich minerals from the Gördes basin (Western Anatolia, Turkey) was investigated by conducting experiments and analyzing data for different kinetic models.

2. Materials and methods

2.1. Sample preparation and characterization

Clinoptilolite-rich minerals were obtained from the Gördes region of Western Anatolia Turkey. The minerals were mainly made up of clinoptilolite (80–85%), and quartz (5–10%), analcime + mordenite (<5%) [32]. The clinoptilolite-rich mineral samples were ground, wet settled and sieved to remove soluble impurities. Thereafter the samples were dried in an oven at 200 °C for 3 h. Brunauer–Emmett–Teller (BET) surface area and micro and mezzo pore size distribution of the samples were determined by N_2 adsorption performed at 77.45 K with a Micromeritics ASAP 2010 static volumetric adsorption instrument after degassing at 350 °C and 10^{-5} mbar for 24 h. The surface morphology and macropore size of clinoptilolite-rich minerals were estimated with a Phillips XL30S FEG electron microscope. Chemical composition (by ICP–AES 96, Varian), mineralogy and crystallinity (by X-Pert Pro, Philips), IR characterization (by FTIR-8201, Shimadzu) and Thermogravimetric (by TGA-51/51H, Shimadzu) analyses were performed as previously described [17]. Zeta potential measurements of the mineral samples were measured using 5 mg/mL samples in potassium phosphate buffer solution at pHs 5.5, 6.8 and 8 with a Zetasizer 3000 HAS analyzer (Malvern Instruments), where pH 6.8 is the optimum pH for GUS activity (recommended by the purchaser instructions) and pH 5.5–8 is the pH range simulating the fasted and fed states of gastrointestinal media.

The GUS enzyme (EC 3.2.1.31, with a molecular weight of 290 kDa from Sigma-Aldrich Chemical Company, Germany) used in this study was of bacterial origin (*E. coli*). Enzyme working solutions were prepared from the GUS enzyme with a 100 μg/mL concentration in potassium phosphate buffer solution at pHs 5.5, 6.8 and 8. The size distribution of the enzyme was measured with a Zetasizer 3000 HAS analyzer (Malvern Instruments).

2.2. Batch adsorption studies

To study the possibility of the eliminating the GUS enzyme by clinoptilolite-rich minerals in the gastrointestinal system, batch adsorption experiments, which were designed to simulate gastrointestinal conditions (37 °C, pH 5.5–8), were performed. Optimum conditions for GUS activity (from an *E. coli* source), 37 °C and pH 6.8, were also considered. The experimental parameters, including the amount and particle size of clinoptilolites, initial enzyme concentration, shaking rate, pH and temperature are shown in Table 1. Potassium phosphate buffer solution (10 mL) of was placed into a 25 mL conical flask, and experiments were performed for the specified GUS concentrations and clinoptilolite amount. Flasks were placed in an orbital shaking water bath for 150 min which was more than ample time for equilibrium. 100 μL of sample was removed from each flask to estimate the enzyme concentration at specific time intervals; mineral free samples were used as control. Samples were analyzed spectrophotometrically using a microplate reader (Varioscan, Thermo) at 255 nm which is the wavelength of the maximum absorbance of GUS. To determine the GUS concentration, a standard curve (GUS concentration vs. absorbance) was plotted for various GUS concentrations in the range of 0–500 μg/mL. Adsorption experiments were performed in triplicate, and mean values were used for adsorption analyses. The amount of enzyme adsorbed was calculated by mass balance as follows:

$$q_t = \frac{V(C_o - C_t)}{m} \quad (1)$$

where C_o is the initial enzyme concentration (μg/mL), C_t is the enzyme concentration in the solution at any time t (μg/mL), q_t is the concentration of GUS (μg/mg) at time t in the adsorbed phase, V is the volume of the solution (mL) and m is the mass of the clinoptilolite (mg).

2.3. Modeling of adsorption kinetic and equilibrium data

The transport of GUS from the gastrointestinal media to the clinoptilolite particle surface through an external film and, subsequent diffusion from the external surface to internal sites through the pores of the particle (intraparticle diffusion; pore diffusion surface diffusion) and adsorption of GUS on the mineral active sites are three consecutive steps during the process. Although all of these steps are effective during the process, the overall rate of adsorption may be controlled by the one that is the slowest. Theoretical analysis of adsorption by particle yields complicated mathematical relationships that were provided and solved by Barrer [33], Boyd [34] and Crank [35]; for some special cases. Considering the complexity of the adsorption process, various simplified models have been reported in the literature and each model has its own limitations due to their simplifying assumptions. Spherical adsorbent particles in an infinite volume of dilute solutions (linear isotherm equilibria) with constant temperature and diffusivity are usually used in simplified models such as in existing study.

With a substantial understanding of the kinetic and equilibrium constants, one can identify the ideal temperatures for system and predict the rates of process for the elimination of GUS, which will lead to optimize design outcomes (higher yield, faster rate) under simulated intestinal conditions. Therefore, the adsorption equilibria and kinetic models constants are critical design variables to estimate the performance and to predict the mechanism of an adsorption process. In this study to investigate the mechanism of adsorption, rate constants were determined by external film diffusion, intraparticle diffusion and pseudo 1st and 2nd order reaction models. In the description of adsorption equilibria Langmuir and Freundlich isotherm models were applied.

2.3.1. Diffusion models

2.3.1.1. External mass transfer or surface resistance control. If diffusion within an adsorbent particle is very rapid or if the adsorbent is nonporous, adsorption can be considered to occur only on the external surface, while diffusion through the laminar film surrounding a particle controls diffusion. Thus, in this analysis, the relationship given by Boyd [34] may be used:

$$\frac{\bar{q}}{q_\infty} = 1 - e^{[-(3k_f t)/(KR_p)]} \quad (2)$$

where the value of average adsorbed phase concentration q is presented as $\bar{q}$ at any time t (μg/mg), q_∞ is the equilibrium adsorbed phase concentration (μg/mg), k_f is the external mass transfer coefficient (m/min), R_p is the average particle diameter (m), K is the initial slope of the isotherm at the specified temperature (mL/mg). For cases in which mass transfer is controlled by surface/skin resistance, an analogous relationship in which the external film diffusion coefficient k_f is replaced by $k_s = D_s/\delta$, the ratio of the

Table 1
Experimental parameters for GUS adsorption by clinoptilolite rich mineral.

Parameter	Initial GUS concentration (μg/mL)	Shaking rate (rpm)	pH	Particle size (μm)	Solid liquid ratio (S/L: mg/mL)	Temperature (°C)
Initial GUS Concentration (μg/mL)	20, 50, 100, 150, 200, 300, 500	150	6.8	45–75	5	37
Shaking rate (rpm)	100	50, 100, 150	6.8	45–75	5	37
pH	100	150	5.5, 6.8, 8	45–75	5	37
Particle size (μm)	100	150	6.8	75–106, 45–75, 25–45	5	37
Solid liquid ratio (S/L: mg/mL)	100	150	6.8	45–75	3, 5, 10	37
Temperature (°C)	100	150	6.8	45–75	5	15, 25, 37

effective diffusivity and thickness of the solid surface film. k_f or k_s is determined from the initial slope of the– $\ln[1-(\bar{q}/q_\infty)]$ vs. t plot and the straight line, which passes through the origin and, indicates external film diffusion or surface/skin resistance control [36].

2.3.1.2. Intraparticle diffusion. The most extensive model used for intraparticle diffusion controlling cases is the one provided by Weber Morris [37], which is actually a simplification of Crank's solution based on the Fick's second law:

$$q_t = k_d t^{0.5} \tag{3}$$

A plot of adsorbate concentration against the square root of time should be linear and pass through the origin, where q_t is the adsorbed phase concentration at any time t (μg/mg), k_d is the diffusion rate constant (μg/mg min$^{0.5}$), t is time (min). Plots of adsorbed phase concentration vs. the square root of time should be linear, and this was used to determine k_d.

2.3.2. Reaction models

2.3.2.1. Pseudo first order model. The 1st order reaction model is known as the Lagergren equation which is the earliest model describing the adsorption rate with respect to adsorption capacity. This model includes all of the steps in the adsorption process including external diffusion, pore diffusion and binding to active sites [38]. The model assumes that the change in the adsorbed phase concentration with time is directly proportional to the difference between the equilibrium concentration and adsorbed phase concentration at any time t [39]. The model is represented as follows:

$$\frac{dq_t}{dt} = k_1(q_e - q_t) \tag{4}$$

where k_1 is the 1st order reaction rate constant (min^{-1}), q_e and q_t are the adsorbed phase concentrations at equilibrium and at any time t in μg/mg, respectively. The integrated form of the equation is as follows:

$$\ln(q_e - q_t) = \ln\ q_e - k_1 t \tag{5}$$

$\ln(q_e - q_t)$ vs. t plot was used in the determination of k_1.

Considering the similarity in the external film diffusion or surface resistance control and Lagergren Pseudo First Order Model equations, the rate parameter obtained from the slope will be either a rate constant for the mass transfer or adsorption reaction or their combination. Distinction between these results will be difficult, although surface skin or film diffusion will have much stronger dependence on agitation. According to the studies performed by Boyd et al. [34], if the reaction is the controlling one, the slope will vary by concentration and temperature only, while for the surface film diffusion control it will vary with the particle size and shaking rate.

2.3.2.2. Pseudo second order model. The pseudo second-order reaction model assumes that the adsorbed phase concentration changes over time are directly proportional to the square of the difference between the equilibrium concentration and adsorbed phase concentration at any time t. The equation is expressed in [40]:

$$\frac{dq_t}{dt} = k_2(q_e - q_t)^2 \tag{6}$$

where k_2 is the rate constant of the pseudo second-order (μg/mg min); and q_e and q_t are the adsorbed phase concentrations at equilibrium and at any time t in μg/mg, respectively. The equation can be rearranged to obtain:

$$\frac{t}{q_t} = \left(\frac{1}{k_2 q_e^2}\right) + \left(\frac{1}{q_e}\right) t \tag{7}$$

The plot of (t/q_t) against t represents a linear relationship from which q_e and k_2 were determined from the slope and intercept of the plot, respectively.

2.4. Adsorption equilibria

Adsorption equilibria can be expressed by adsorption isotherm relationships based on the data in the adsorption experiments performed. Two isotherm models, Langmuir and Freundlich, which are commonly used, were tested. The Langmuir isotherm model is represented by the following equation that model assumes that adsorption take place on energetically uniform and identical surface sites:

$$q_e = \frac{q_m K_L C_e}{1 + K_L C_e} \tag{8}$$

C_e (μg/mL) is the adsorptive concentration in solution at equilibrium, q_e (μg/mg) is the amount of adsorptive adsorbed per unit mass of sorbent at equilibrium, q_m (μg/mg) and K_L (mL/mg) are the maximum sorption capacity and Langmuir constant, respectively. The maximum sorption capacity and Langmuir constant were determined from the slope and intercept of the C_e/q_e vs. C_e plot, respectively.

The Freundlich isotherm is empirical and a special case for heterogeneous surface energies [41,42]. The expression is an exponential equation, and the isotherm model assumes that an infinite amount of adsorption can theoretically occur:

$$q_e = K_F C_e^{1/n} \tag{9}$$

where C_e (μg/mL) is the adsorptive concentration in solution at equilibrium, q_e (μg/mg) is the amount of adsorptive adsorbed per unit mass of sorbent at equilibrium, K_F is the Freundlich constant and $1/n$ is the heterogeneity factor. The equation may also be written in the logarithmic form, and the values for K_F and n were calculated from the slope and intercept of the linear $\ln C_e$ vs. $\ln q_e$ plot, respectively.

2.5. Thermodynamic analysis

The thermodynamic parameters of adsorption, Gibbs free energy change (ΔG°), standard enthalpy change (ΔH°), and

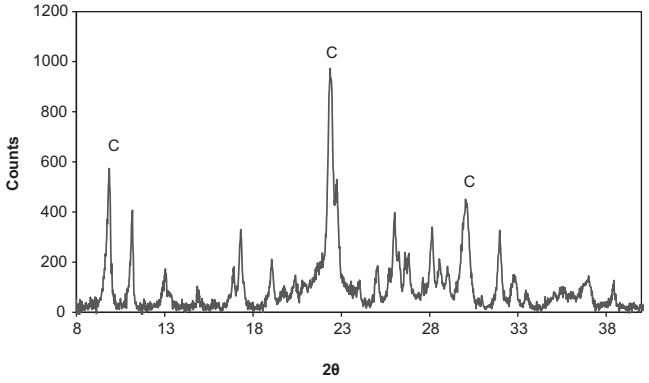

Fig. 1. XRD patterns of clinoptilolite rich mineral (C: characteristic clinoptilolite peaks, powder particle size: 45–75 μm).

standard entropy change (ΔS°) provide information concerning the type and mechanism of the adsorption process. The Gibbs free energy change in adsorption (ΔG°) indicates whether it is spontaneous, and a higher negative value indicates more energetically favorable cases. These values were calculated based on data from designated experiments. The free energy change (ΔG°) is given by:

$$\Delta G^\circ = -RT \ln K = \Delta H^\circ - T\,\Delta S^\circ \quad (10)$$

where R is the universal gas constant, 8.314 J/mol K, K is the equilibrium constant and T is the absolute temperature. The slope and intercept of the $\ln K$ vs. $1/T$ plot was used to determine ΔH° (kJ/mol) and ΔS° (kJ/mol K), respectively. A negative enthalpy value change (ΔH°) indicates an exothermic process.

The activation energy of GUS adsorption for clinoptilolite-rich minerals was calculated using the Arrhenius relationship:

$$\ln\ k = \ln A_a - \frac{E_A}{RT} \quad (11)$$

where A_a is the frequency factor for adsorption, E_A (kJ/mol) is the activation energy of adsorption and k is the pseudo second order rate constant. E_A was determined from the slope of the $\ln k$ vs. $1/T$ plot.

3. Results and discussion

3.1. Characterization results

XRD results for clinoptilolite rich-minerals showed that characteristic clinoptilolite peaks were recognized at nearly $2\theta = 9.8^\circ$, 22.3° and 30° (Fig. 1) and the purity of the samples was found to be 90% using the quantitative analysis method [43]. The chemical composition of the sample was; 73.4 SiO_2, 14% Al_2O_3, 2.5% Fe_2O_3, 4.6% K_2O, 1.8% Na_2O, 2.2% CaO, 1.1% MgO and 13.3% H_2O. The BET surface area was found to be 41.7 m^2/g.

The pore size distribution of the clinoptilolite-rich minerals samples was found to be in the range of 0.54–300 nm by using the volumetric system. SEM pictures of the clinoptilolite samples were used to estimate of the pore structures and macroporous morphologies among the clinoptilolite crystals [44]. The results in Fig. 2 show that the macropore sizes of the crystals range between 784 and 4400 nm. GUS has a tetramer structure with high molecular weight of 290 kDa and its size distribution results showed that its size varied in the range of 60–120 nm in sorption solution (Fig. 3).

3.2. Effect of experimental parameters on GUS adsorption

The accessibility of the GUS enzyme to the available active sites is restricted by the pore/channel dimensions of the mineral particles, which are composed of clinoptilolite crystals with micropores,

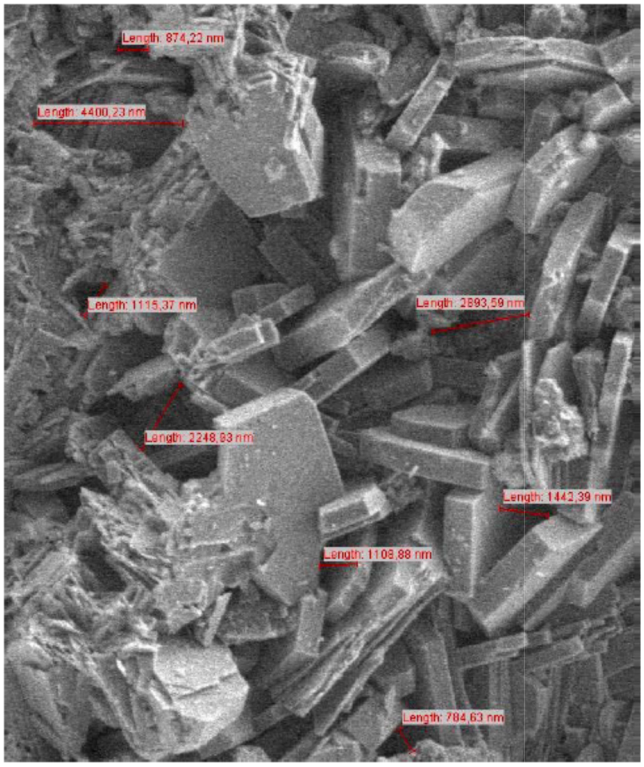

Fig. 2. SEM image clinoptilolite rich mineral and macropore sizes (powder particle size: 45–75 μm).

mesopores and macro pores in the crystals. The size distribution results for GUS implied that the enzyme could not go through the micropores of the crystals, which are in the 0.4–0.5 nm range. Due to the possible coexistence of several orientations in the working solution [45], the dynamic behavior of GUS might change during the adsorption process. Thus, terminals on GUS can bend and may diffuse through the mezzo and macro pores of the particles, which are large enough for GUS to diffuse into.

3.2.1. Effect of initial GUS concentration

Figs. 4 and 5 show the effect of contact time on the amount of GUS removed from the simulated gastrointestinal fluid and adsorbed by the clinoptilolite-rich minerals, respectively. For different initial GUS concentrations, the initial minutes appear to be related to the surface film resistance, and subsequent intraparticle diffusion through the macro pores is also involved. The rate slows with adsorption progression due to the decreasing

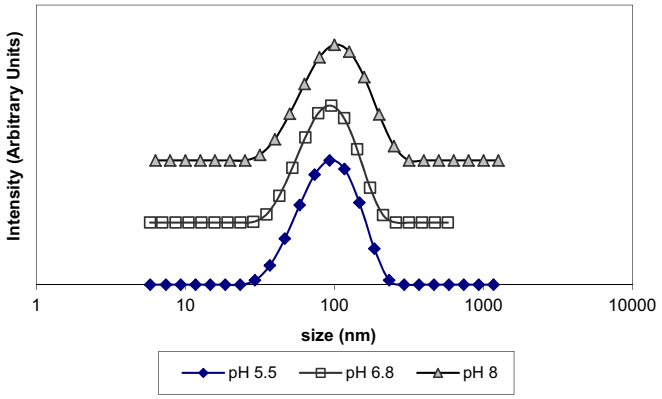

Fig. 3. Size distribution of GUS (100 μg/mL, 37 °C, pH 5.5–6.8–8).

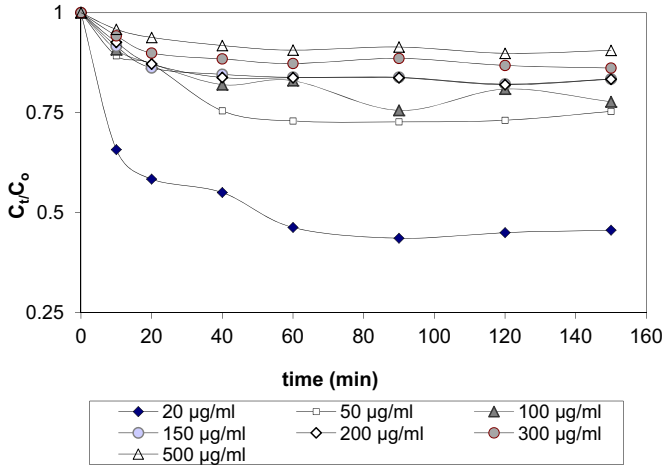

Fig. 4. Concentration decay curves at various initial GUS concentrations (C_i: 20–500 µg/mL, 37 °C, 150 rpm, S/L: 5 mg/mL, pH 6.8, particle size: 45–75 µm).

numbers of unoccupied active sites, and equilibrium is finally attained with saturation. Increased initial concentrations result in higher concentration differences between the clinoptilolite particle surface and simulated gastrointestinal medium, leading to an increase in adsorption rates due to a higher driving force for overcoming the mass transfer resistances. A similar trend was observed for all concentrations. The results showed that the GUS removal percentage changed within the range of 9.4–54.4% depending on its initial concentration.

3.2.2. Effect of solution pH

The effect of solution pH on adsorption kinetics and equilibria is shown in Fig. 6. pH influences the protonation or deprotonation of surfaces during the sorption process. The active sites on the clinoptilolite-rich mineral surface are Si—OH and Al—OH groups. With increases in pH, ≡Si—O^- and ≡Al—O^- groups are more dominant, and results from zeta potential measurements indicated that clinoptilolite was negatively charged at three pH values (Table 2). For the GUS enzyme, the isoelectric point (pI) is 4.8, and GUS should have a net negative charge at all three pH values. An increase in pH resulted in an increase in the adsorbed amount, which was 7 times higher for pH 8 and increased from 1.19 to 8.46 µg/mg for the pH 5.5 and 8.0, respectively. At pH 8, positively charged amino acids may become more exposed to the surface yielding higher adsorbed amount due to possible conformational change with the

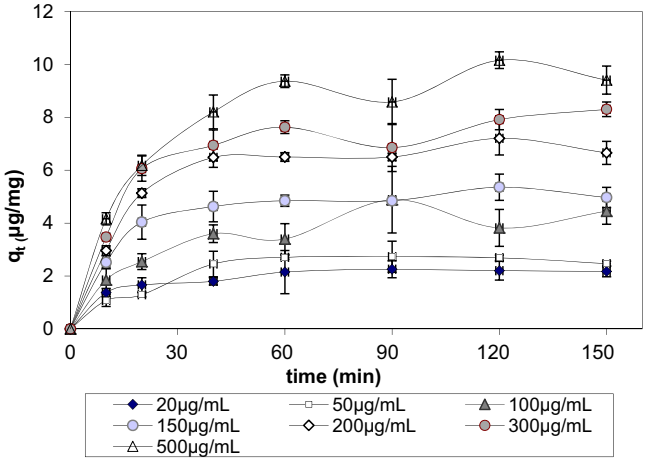

Fig. 5. Uptake curves for GUS adsorption by clinoptilolite rich mineral (37 °C, 150 rpm, S/L: 5 mg/mL, pH 6.8, particle size: 45–75 µm).

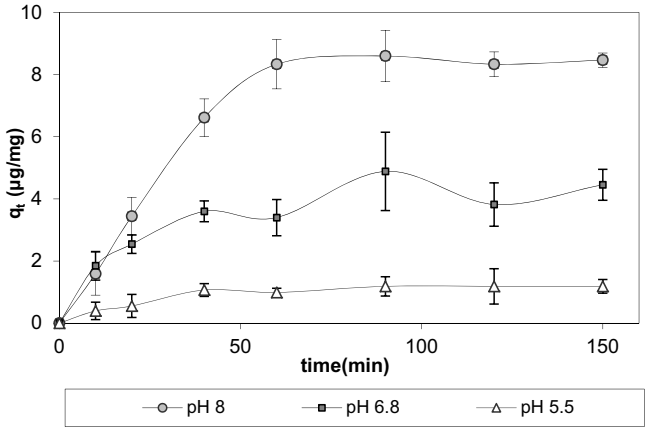

Fig. 6. Effect of pH on adsorption kinetics of GUS by clinoptilolite rich mineral (37 °C, S/L: 5 mg/mL, C_i: 100 µg/mL, 150 rpm, particle size: 45–75 µm).

loss in the stability of enzyme at pH 8 [46]. GUS may interact with clinoptilolite-rich minerals through substitution of the ionized carboxyl base, and negative charges (repulsion) would influence binding at the basic side above the pI. This situation indicates that hydrophobic interactions could be more important for the adsorption process above the pI. It was reported that proteins cannot bind to silicalite (which has no Al), where Al molecules in zeolites may play a role in adsorption and above the pI, although there was electrostatic repulsion, some zeolites such as H-USYs were found to efficiently adsorb biopolymers [47]. This case was explained by the carboxylate anions on the protein structure, which could be substitute for water coordinating with metal ions, and the negative charges on proteins might result in the substitution of water at the Lewis acid sites of Al. Therefore, in addition to hydrophobic interactions, contributions from water substitution reactions may be important in the adsorption mechanism.

3.2.3. Effect of shaking rate

Shaking rate is important for the establishment of homogenous GUS concentrations in bulk medium. In addition, shaking rate affects the thickness of the surface film layer surrounding clinoptilolite mineral particles. Experiments performed with several sorbent–sorbate pairs demonstrate surface film diffusion, which has a strong dependence on the shaking rate; as the only rate controlling step for the first few minutes [40]. Fig. 7 shows the effects of the shaking rate on the amount of GUS adsorbed against the contact time. As observed in the figure, the initial uptake rate increased with increasing shaking speed. This result may imply that external diffusion resistance is likely to have more significant effects at the early stages of adsorption. Because the external diffusion resistance is proportional to the film thickness via, the increasing shaking rate, the external diffusion resistance becomes smaller due to a reduction in the thickness of the boundary layer. Although it was expected to have same adsorbed amounts at equilibrium for all shaking rates; at 50 and 100 rpm, an equilibrium amount for 150 rpm could not reached. This appears to be related to the clogging of the pores by surface blocking, which occurs on the particle surface by the heavy GUS molecule. Only after a critical force is

Table 2
Variations in the zeta potential of clinoptilolite rich mineral (S/L: 5 mg/mL, 37 °C, pH 5.5; 6.8 and 8, particle size: 45–75 µm).

pH values	Zeta potential values (mV)
5.5	−11.02
6.8	−13.53
8	−15.33

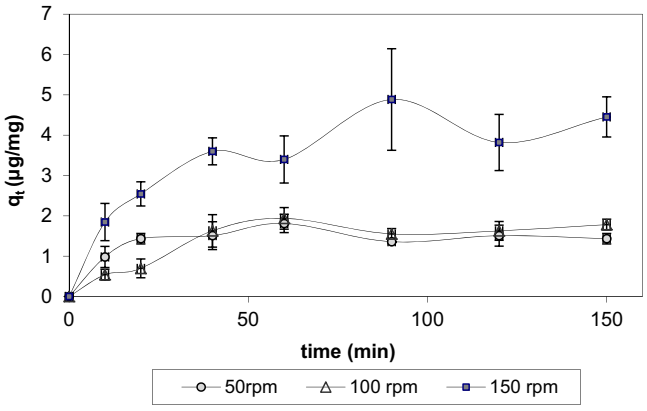

Fig. 7. Effect of shaking rate on adsorption kinetics of GUS by clinoptilolite rich mineral (37 °C, S/L: 5 mg/mL, C_i: 100 μg/mL, pH 6.8, particle size: 45–75 μm).

created by the fluid movement around the particle can it be removed and become possible for the GUS molecule to diffuse through the pores.

3.2.4. Effect of particle size

Considering the sizes of the GUS molecule and clinoptilolite crystals, diffusion of GUS into the micropores of the crystals is not possible, and adsorption is almost limited by the external surface together with the macropores of the clinoptilolite crystals. The effects of particle size on the adsorption kinetics are shown in Fig. 8. The results show that initial uptake rates and amount of enzyme adsorbed at equilibrium increase with decreases in particle size, particularly for finer particles (<45 μm). Grinding large particles to smaller particles opens clogged pores and channels. Moreover, smaller particle sizes provide greater surface area, higher numbers of active sites become available for adsorption for a given mass of minerals.

3.2.5. Effect of adsorbent concentration

The effects of the amount of clinoptilolite rich-minerals; solid liquid ratio (S/L), on the adsorption kinetics are shown in Fig. 9. Although an increase was observed in the total amount of GUS adsorbed with increases in the amount of minerals due to the existence of greater surface area and number of active sites provided, the amount adsorbed per mg of mineral increased up to a critical value. The maximum adsorbed amount of enzyme per unit mass of mineral did not significantly change when the adsorbent concentration was increased from 5 to 10 mg/mL. This result may be attributed

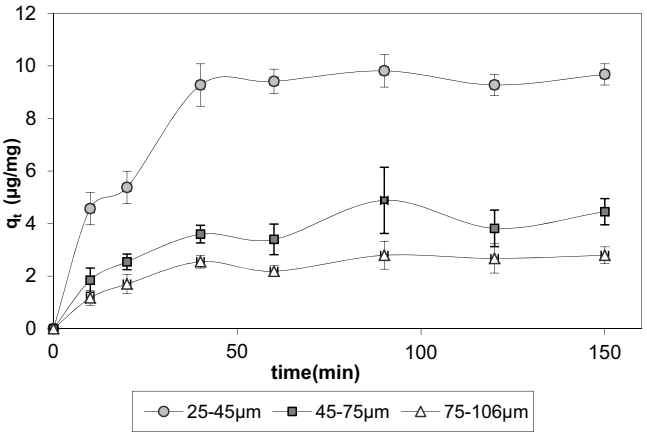

Fig. 8. Effect of particle size on adsorption kinetics of GUS by clinoptilolite rich mineral (37 °C, S/L: 5 mg/mL, C_i: 100 μg/mL, pH 6.8, 150 rpm).

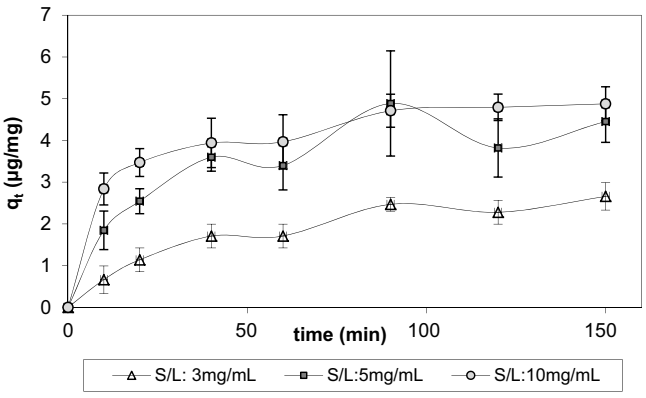

Fig. 9. Effect of solid liquid ratio on adsorption kinetics of GUS by clinoptilolite rich mineral (37 °C, 150 rpm, C_i: 100 μg/mL, pH 6.8, particle size: 45–75 μm).

to complex interactions at higher mineral concentrations. Higher mineral concentrations might trigger interactions such as collisions of adsorbents thus, adsorbed amounts are negatively affected or there may be partial overlapping or aggregation of adsorbent at higher concentrations where total surface area and the availability of sorption sites were reduced. A similar behavior was observed by several investigators [48,49].

3.2.6. Effect of temperature

The results of the effects of temperature on the adsorption kinetics are shown in Fig. 10. The results indicated that the adsorption capacity of clinoptilolite rich-minerals increase with a decrease in temperature, which implying an exothermic nature of adsorption. At 15 °C and 25 °C, there was no considerable difference in the adsorption behavior of the mineral. In contrast, at 37 °C, adsorption capacity was considerably reduced, which may be attributed to conformational changes or aggregation of the GUS molecule and blockage of the surface.

3.3. Kinetic model results and adsorption mechanism

The values of the external diffusion coefficients (k_f), intraparticle diffusion rate constants (k_d), and pseudo first-order (k_1) and second-order (k_2) rate constants are tabulated in Tables 3–7 for the different experimental parameters. Slight fluctuations in k_f values, which did not show a consistent trend, were obtained with an increase in the initial concentration (Table 3). Because the adsorbent is a natural clinoptilolite-rich mineral, this might be attributed to the structural behavior [38] or possible interactions of the

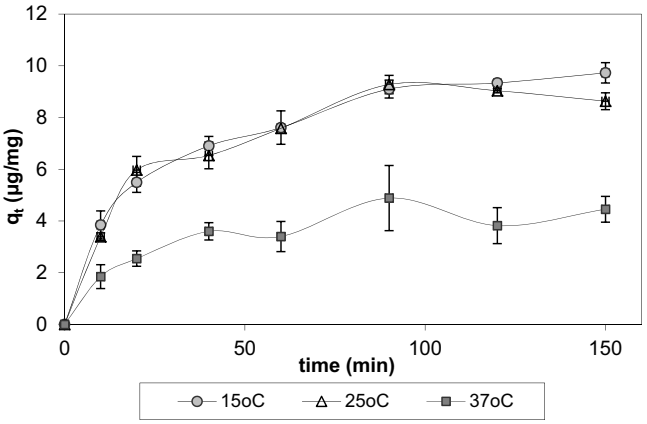

Fig. 10. Effect of temperature on adsorption kinetics of GUS by clinoptilolite rich mineral (S/L: 5 mg/mL, 150 rpm, C_i: 100 μg/mL, pH 6.8, particle size: 45–75 μm).

Table 3
Effect of initial GUS concentration on kinetic model parameters (37 °C, 150 rpm, S/L: 5 mg/mL, pH 6.8, particle size: 45–75 μm).

Concentration (μg/mL)	$k_f \times 10^8$ (m/min)	r^2	k_d (μg/mg min$^{0.5}$)	r^2	$k_1 \times 10^2$ (min^{-1})	r^2	$k_2 \times 10^2$ (mg/μg min)	r^2
20	1.56	0.977	0.132	0.906	2.28	0.958	5.88	0.964
50	0.87	0.893	0.162	0.806	6.77	0.930	2.75	0.932
100	0.89	0.910	0.555	0.868	3.78	0.917	1.27	0.919
150	2.25	0.962	0.641	0.826	6.26	0.945	2.39	0.965
200	2.37	0.975	0.761	0.818	10.32	0.963	1.47	0.964
300	1.97	0.942	1.055	0.856	3.96	0.927	0.91	0.949
500	2.09	0.977	1.266	0.881	8.36	0.972	0.74	0.972

Table 4
Effect of shaking rate on kinetic model parameters (C_i: 100 μg/mL, 37 °C, 150 rpm, S/L: 5 mg/mL, pH 6.8, particle size: 45–75 μm).

Shaking rate (rpm)	$k_f \times 10^8$ (m/min)	r^2	k_d (μg/mg min$^{0.5}$)	r^2	$k_1 \times 10^2$ (min^{-1})	r^2	$k_2 \times 10^2$ (mg/μg min)	r^2
50	0.56	0.456	0.1523 C_d[a]: 0.5932	0.427	10.41	0.674	57.61	0.736
100	0.84	0.852	0.1184 C_d: 0.1683	0.785	7.32	0.903	2.08	0.890
150	0.89	0.910	0.5554 C_d: 0.0789	0.868	3.78	0.917	1.27	0.919

[a] C_d: intercept of the q_t vs. square root of time plot.

Table 5
Effect of pH on kinetic model parameters (C_i: 100 μg/mL, 37 °C, 150 rpm, S/L: 5 mg/mL, particle size: 45–75 μm).

pH	$k_f \times 10^8$ (m/min)	r^2	k_d (μg/mg min$^{0.5}$)	r^2	$k_1 \times 10^2$ (min^{-1})	r^2	$k_2 \times 10^2$ (mg/μg min)	r^2
5.5	2.75	0.892	1.598	0.888	4.47	0.975	2.39	0.981
6.8	0.89	0.91	0.555	0.868	3.78	0.917	1.27	0.919
8	0.96	0.910	0.217	0.895	6.61	0.965	1.47	0.967

Table 6
Effect of particle size on kinetic model parameters (C_i: 100 μg/mL, 37 °C, 150 rpm, S/L: 5 mg/mL, pH 6.8).

Particle size (μm)	$k_f \times 10^8$ (m/min)	r^2	k_d (μg/mg min$^{0.5}$)	r^2	$k_1 \times 10^2$ (min^{-1})	r^2	$k_2 \times 10^2$ (mg/μg min)	r^2
25–45	1.63	0.958	1.20	0.833	8.94	0.946	0.85	0.946
45–75	0.89	0.91	0.555	0.868	3.78	0.917	1.27	0.919
75–106	1.29	0.945	0.217	0.884	6.49	0.954	2.14	0.954

Table 7
Effect of temperature on kinetic model parameters (C_i: 100 μg/mL, 150 rpm, S/L: 5 mg/mL, pH 6.8 particle size: 45–75 μm).

Temperature (°C)	$k_f \times 10^8$ (m/min)	r^2	k_d (μg/mg min$^{0.5}$)	r^2	$k_1 \times 10^2$ (min^{-1})	r^2	$k_2 \times 10^2$ (mg/μg min)	r^2
15	10.63	0.979	0.954	0.977	2.65	0.996	0.46	0.987
25	7.85	0.968	0.592	0.948	2.14	0.978	0.85	0.975
37	0.89	0.910	0.554	0.868	3.78	0.917	1.27	0.919

functional groups of GUS molecule with each other. Table 3 illustrates that the k_d values were increased within the same order of magnitude as the increase in the GUS concentration, which could be attributed to the driving force of diffusion. The results indicated that intraparticle diffusion was not the sole rate-limiting step because plots for q_t vs. $t^{0.5}$ yielded a straight line that did not pass through the origin. However, intraparticle diffusion plots with high correlation coefficients indicate that the presence of the intraparticle diffusion process as one of the rate-limiting steps during adsorption. A similar behavior was observed in several studies of various adsorbent adsorbate pairs [50,51]. In the 2nd order model, although the k_2 values showed a decreasing trend with increases in the initial concentration up to 150 μg/mL, the tendency was not consistent. At low initial concentrations, GUS bound to high-energy sites on the clinoptilolite-rich mineral surface at the early stages of the adsorption. Then, low-energy sites could be occupied by GUS with increases in its initial concentration. Thus, higher rate parameters for the pseudo-second order were achieved [50], and some conformational changes of GUS may also be effective.

It can be seen in Table 4 that k_f values increased with increases in the shaking rate. Because the external diffusion resistance is proportional to the surface film/skin resistance, at higher shaking rates with decreases in external thickness or the elimination of the surface skin, external diffusion resistance was reduced, and clogged pores were opened. C_d, the intercept of the q_t vs. square root of time plot, is proportional to the external film/surface skin thickness. Higher intercept values for 50 and 100 rpm indicated a contribution of external film/skin resistance at lower rpm values. A similar case was reported in the literature for different pairs [8,52].

The adsorption of GUS from aqueous solutions onto the surface of clinoptilolite rich-minerals was highly solution pH dependent; it was affected by both of the surface properties of the sorbent and the GUS structure. The results implied that the effects of pH on kinetic model parameters were irregular (Table 5). Fluctuations in the kinetic model parameters might be attributed to the protein structure of the enzyme. The dynamic conformation change of the enzyme with pH most likely caused alterations in the charge and orientation of the enzyme.

Table 6 illustrates that external diffusion coefficient demonstrated no consistent trend with the increase in particle size. This result might be attributed to the dynamic behavior of the GUS molecule. With the increase in particle size, the surface area of the particle decreased and the large GUS molecules might have showed a tendency to occupy the surface, and they might interact with each other. The k_d values decreased with increases in particle size because the time and pathway required for diffusion the interior parts of the clinoptilolite-rich mineral increased. The amount

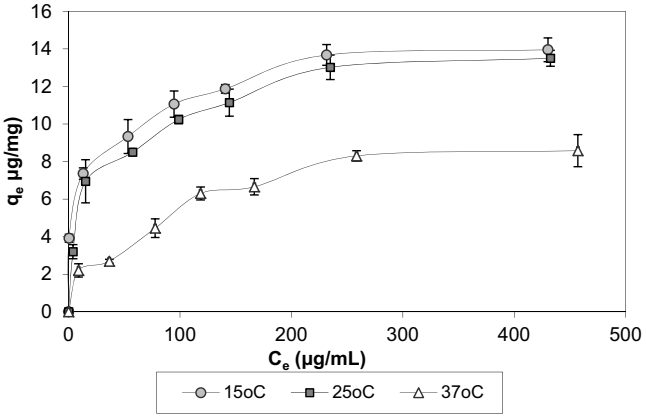

Fig. 11. Adsorption isotherms at 15, 25 and 37 °C (S/L: 5 mg/mL, 150 rpm, pH 6.8, particle size: 45–75 µm).

of the external surface area available for a rapid reaction decreases with increasing particle size for a constant sorbent mass.

The results in Table 7 show that the 1st and 2nd order reaction rate parameters increased with temperature. However, the k_f and k_d values decreased with increases in temperature, and the decrease was particularly significant for k_f. This finding indicated that increasing temperature does favor the sorption process in which the diffusion rate of GUS molecules thorough particle surfaces and into the pores of the particle decreased due to increases in skin resistance and blocking of the surface. For example, at higher temperatures, GUS molecules might undergo conformational changes; thus free amino acid residues exposed to the surface might have changed. It was reported that some protein molecules, at temperatures higher than room temperature, may aggregate by S—S (disulfide) bond formation [45]. Additionally, aggregation of the terminals might occur due to attractive electrostatic interactions with the oppositely charged groups by changes in conformation with temperature to a more suitable form for electrostatic interaction. Thus, the aggregation of GUS in solution may result a molecular form with a bigger size; blocks the surface and increases surface skin resistance.

3.4. Sorption isotherm model results

The isotherms and related constants are shown in Fig. 11 and Table 8, respectively. The Langmuir model, which is based on monolayer coverage, demonstrated superiority over the Freundlich model, particularly for higher temperatures. Sorption equilibrium data were well represented by the Langmuir isotherm model with higher correlation coefficients and higher values for K_L signifying higher affinity for GUS binding. K_L decreased with increasing temperature so that the low temperature adsorption process is more favorable.

3.5. Thermodynamic parameters and activation energy

The thermodynamic parameters: standard free energy change (ΔG°), enthalpy change (ΔH°), and entropy change (ΔS°) were evaluated to test the feasibility, heat effect, and mechanism of the removal of GUS from the simulated intestinal media by the adsorption process. The results of the thermodynamic parameters are shown in Table 9. The ΔG° values for GUS were negative, demonstrating that free energy decreased with adsorption. Free energy changes give idea about the feasibility of the adsorption process. GUS adsorption was found to be spontaneous at the temperatures under investigation (288–310 K) as indicated from the negative ΔG° values. A negative value for entropy changes indicates that degree of freedom decreases at the solid/liquid interface during adsorption. The results with negative values for enthalpy changes indicated that the adsorption of GUS on clinoptilolite minerals was an exothermic process.

Although physical or chemical nature of adsorption can usually be estimated by comparing the standard enthalpy change (ΔH°), the Gibbs free energy change (ΔG°) and activation energy values with values reported in the literature, a clear distinction is not easy. For chemical adsorption, the release of heat is much larger than the heat of condensation and enthalpy changes were reported to be in the range of 10–30 kJ/mol, whereas for chemical adsorption, it is over and generally falls in the range of 80–200 kJ/mol [36,53,54]. Activation energies less than 42 kJ/mol were attributed to physical processes, and higher activation energies (>42 kJ/mol) were attributed to chemical processes; generally, 0 to −20 kJ/mol for free energy change was reported to be the physical range, and −80 to −400 kJ/mol was reported to be the range for chemical adsorption [55,56]. All values for the thermodynamic parameters for GUS adsorption were well below the values for chemical adsorption (the value of activation energy for GUS adsorption was 34.1 kJ/mol, enthalpy change was −46.89 kJ/mol, ΔG° was in the range of −21.36 to −23.15 kJ/mol), indicating physical rather than chemical adsorption.

Table 8
Langmuir and Freundlich constants for GUS adsorption.

Temperature (°C)	Langmuir isotherm			Freundlich isotherm		
	q_m (µg/mg)	K_L (mL/mg)	r^2	K_F (µg/mg)	1/n	r^2
15	14.41	54.60	0.995	4.57	0.19	0.994
25	14.20	36.79	0.994	2.52	0.30	0.940
37	10.00	13.73	0.976	1.01	0.36	0.902

Table 9
Thermodynamic parameters for GUS adsorption by clinoptilolite rich mineral.

ΔH° (kJ/mol)	ΔS° (J/mol K)	ΔG° (kJ/mol)		
		T = 288 K	T = 298 K	T = 310 K
−46.89	−81.68	−23.15	−22.98	−21.36

4. Conclusions

In this study, the adsorption of bacterial β-glucuronidase, which is thought to be responsible for the production of reactive metabolites related to some diseases and cancer development, by clinoptilolite-rich mineral under simulated gastrointestinal conditions was investigated. Kinetic studies indicated that initial GUS concentrations lead to an increase in adsorption capacity and rate. The removal percentage of GUS by clinoptilolite-rich minerals ranged between 9.4 and 54.4%, depending on its initial concentration. Higher adsorption capacities and rates were achieved with increases in shaking rates. It was found that when the adsorption temperature was increased, the adsorption capacity was decreased. The results imply that external film and intraparticle diffusion appear to be effective in GUS adsorption. Sorption isotherm results indicated that the experimental data were well represented by the Langmuir isotherm model. The decrease in adsorption capacity with increasing temperature and low value (magnitude value) for activation energy (E_A) indicated that the adsorption of GUS by clinoptilolite-rich minerals might be by physical adsorption. The negative values for enthalpy change indicated an exothermic process and negative values for the Gibbs free energy change indicated that GUS adsorption was spontaneous at the temperatures studied (288–310 K).

Although clinoptilolite appears to have potential value for eliminating GUS enzyme, further studies at 37 °C and shaking rates simulating gastrointestinal conditions (50–100 rpm) should be performed.

Acknowledgements

This study was supported by the Turkish Republic Prime Ministry State Planning Organization (DPT-2003K120690, Determination of Effects of Zeolite on Health at Cellular and Molecular Level). The authors gratefully acknowledge Prof. Dr. Devrim BALKÖSE and Assist. Prof. Dr. Ayben TOP for their kind contributions.

References

[1] Mumpton F. Uses of natural zeolites in agriculture and industry. Proc Natl Acad Sci U S A 1999;96:3463–70.
[2] Top A, Ülkü S. Silver, zinc, and copper exchange in a Na-clinoptilolite and resulting effect on antibacterial activity. Appl Clay Sci 2004;27:13–9.
[3] Klint D, Eriksson H. Conditions for the adsorption of proteins on ultrastable zeolite Y and its use in protein purification. Protein Expr Purif 1997;10:247–55.
[4] Rivera A, Farias T, Ruiz-Salvador AR, De Menorval LC. Preliminary characterization of drug support systems based on natural clinoptilolite. Microporous Mesoporous Mater 2003;61:249–59.
[5] Rodriguez-Fuentes G, Barrios MA, Iraizoz A, Perdoma I, Cedre B. Enterex: anti-diarrheic drug based on purified natural zeolite clinoptilolite. Zeolites 1997;19:441–8.
[6] Rodriguez-Fuentes G, Denis AR, Alvarez MAB, Colarte AI. Antacid drug based on purified natural clinoptilolite. Microporous Mesoporous Mater 2006;94:200–7.
[7] Narin G, Albayrak ÇB, Ülkü S. Antibacterial and bactericidal activity of nitric oxide-releasing natural zeolite. Appl Clay Sci 2010;50:560–8.
[8] Erdogan BC, Ülkü S. Cr(VI) sorption by using clinoptilolite and bacteria loaded clinoptilolite rich mineral. Microporous Mesoporous Mater 2012;152:253–61.
[9] Hrenovic J, Milenkovic J, Goic-Barisic I, Rajic N. Antibacterial activity of modified natural clinoptilolite against clinical isolates of *Acinetobacter baumannii*. Microporous Mesoporous Mater 2013;169:148–52.
[10] Ortatatlı M, Oğuz H. Ameliorative effects of dietary clinoptilolite on pathological changes in broiler chickens during aflatoxicosis. Res Vet Sci 2001;71:59–66.
[11] Ortatatlı M, Oğuz H, Hatipoglu F, Karaman M. Evaluation of pathological changes in broilers during chronic aflatoxin (50 and 100 ppb) and clinoptilolite exposure. Res Vet Sci 2005;78:61–8.
[12] Oğuz H. A review from experimental trials on detoxification of aflatoxin in poultry feed. Eurasian J Vet Sci 2011;27:1–12.
[13] Topashka-Ancheva M, Beltcheva M, Metcheva R, Heredia-Rojas JA, Rodriguez-De la Fuente AO, Gerasimova T, et al. Modified natural clinoptilolite detoxifies small mammal's organism loaded with lead II: genetic, cell, and physiological effects. Biol Trace Elem Res 2011;147:206–16.
[14] Beltcheva M, Metcheva R, Popov N, Teodorova SE, Heredia-Rojas JA, Rodriguez-De la Fuente AO, et al. Modified natural clinoptilolite detoxifies small mammal's organism loaded with lead I. Lead disposition and kinetic model for lead bioaccumulation. Biol Trace Elem Res 2011;147:180–8.
[15] Rivera A, Rodrigiez-Fuentes G, Altshuler E. Time evolution of a natural clinoptilolite in aqueous medium: conductivity and pH experiments. Microporous Mesoporous Mater 2000;40:173–9.
[16] Pavelic K, Hadzija M. Medical applications of zeolites. In: Auerbach SM, Carrado KA, Dutta PK, editors. Handbook of clinoptilolite rich mineral science and technology. New York: Marcel Dekker Inc.; 2003. p. 143, 1174.
[17] Demirbüker-Kavak D, Ülkü S. Investigation of structural properties of clinoptilolite rich zeolites in simulated digestion conditions and their cytotoxicity against Caco-2 cells in vitro. J Porous Mater 2013;20:331–8.
[18] Zarkovic N, Zarkovic K, Kralj M, Borovic S, Sabovlovic S, Blazi MP. Anticancer and antioxidative effects of micronized zeolite clinoptilolite. Anticancer Res 2003;23:1589–96.
[19] Papaioannou DS, Katsoulos PD, Panousis N, Karatzias H. The role of natural and synthetic zeolites as feed additives on the prevention and/or the treatment of certain farm animal diseases: a review. Microporous Mesoporous Mater 2005;84:161–70.
[20] Tomecková V, Rehák ová M, Mojzišová G, Magura J, Wadsten T, Zelenáková K. Modified natural clinoptilolite with quercetin and quercetin dehydrate and the study of their anticancer activity. Microporous Mesoporous Mater 2012;147:59–67.
[21] Goldin B, Gorbach SL. Alterations in fecal microflora enzymes related to diet, age, *lactobacillus* supplements, and dimethylhydrazine. Cancer 1977;40:2421–6.
[22] De Moreno De Leblanc A, Perdigon G. Reduction of β-glucuronidase and nitroreductase activity by yoghurt in a murine colon cancer model. Biocell 2001;29:15–24.
[23] Beaud D, Tailliez P, Anba-Mondoloni J. Genetic characterization of the β-glucuronidase enzyme from a human intestinal bacterium *Ruminococcus gnavus*. Microbiology 2005;151:2323–30.
[24] Fujisawa T, Aikawa K, Takahashi T, Yamai S, Watanabe K, Kubota Y, et al. Influence of butyric and lactic acids on the β-glucuronidase activity of *Clostridium perfringens*. Lett Appl Microbiol 2001;32:123–5.
[25] Rafter J, Govers M, Martel P, Pannemans D, Pool-Zobel B, Rechkemmer G. Diet-related cancer. Eur J Nutr 2004;2:47–84.
[26] Cardona ME, Norin E, Midtvedt T. β-Glucuronidase activity in germ-free, monoassociated and conventional mice. Microb Ecol Health D 2006;18:38–41.
[27] Dabek M, McCrae SI, Stevens VJ, Duncan SH, Louis P. Distribution of β-glucosidase and β-glucuronidase activity and of β-glucuronidase gene gusin human colonic bacteria. FEMS Microbiol Ecol 2008;66:487–95.
[28] Lampe JW, Li SS, Potter JD, King IB. Serum β-glucuronidase activity is inversely associated with plant-food intakes in humans. J Nutr 2002;132:1341–4.
[29] Devasena T, Menon VP. Fenugreek affects the activity of β-glucuronidase and mucinase in the colon. Phytother Res 2003;17:1088–91.
[30] Demirbüker-Kavak D, Altıok E, Bayraktar O, Ülkü S. *Pistacia terebinthus* extract: as a potential antioxidant, antimicrobial and possible β-glucuronidase inhibitor. J Mol Catal B Enzym 2010;64:167–71.
[31] Lee HW, Choo MK, Bae EA, Kim DH. β-Glucuronidase inhibitor tectorigenin isolated from the flower of *Pueraria thunbergiana* protects carbon tetrachloride-induced liver injury. Liver Int 2003;23:221–6.
[32] Akdeniz Y, Ülkü S. Microwave effect on ion-exchange and structure of clinoptilolite. J Porous Mater 2007;14:55–60.
[33] Barrer RM. Diffusion in and through solids. New York: Cambridge Press; 1941. p. 1–50.
[34] Boyd GE, Adamson AW, Myers Jr LS. The exchange adsorption of ions from aqueous solutions of organic zeolites. II. Kinetics. J Am Chem Soc 1947;69:2836–49.
[35] Crank J. Mathematics of diffusion. Oxford: Clarendon Press; 1970. p. 203–54.
[36] Karger J, Ruthven MD. Diffusion in clinoptilolite rich minerals and other microporous solids. New York: Wiley-Interscience Pubs; 1992. p. 232–6.
[37] Weber WJ, Morris JC. Kinetics of adsorption on carbon from solution. J Sanit Eng Div ASCE 1963;89:31–59.
[38] Chang Y, Chu L, Tsai J, Chiu S. Kinetic study of immobilized lysozyme on the extrudate-shaped NaY zeolite. Process Biochem 2006;41:1864–74.
[39] Lagergren S. About the theory of so-called adsorption of soluble substances. K Sven Vetensk Akad Handl 1898;24:1–39.
[40] Ho YS, Ng JCY, McKay G. Kinetics of pollutant sorption by biosorbents: review. Sep Purif Methods 2000;29:189–232.
[41] Freundlich HM. Uber die adsorption in losungen. Z Phys Chem 1906;57:385–470.
[42] Aksu Z, İşoğlu IA. Removal of copper(II) ions from aqueous solution by biosorption onto agricultural waste sugar beet pulp. Process Biochem 2005;40:3031–44.
[43] Nakamura T, Ishikawa M, Hiraiwa T, Sato J. X-ray diffractometric determination of clinoptilolite in zeolite tuff using multiple analytical lines. Anal Sci 1992;8:539–43.
[44] Kowalczyk P, Sprynskyy M, Terzyk AP, Lebedynets M, Namiesnik J, Buszewski B. Porous structure of natural and modified clinoptilolites. J Colloid Interface Sci 2006;297:77–85.
[45] Nakanishi K, Sakiyama T, Imamura K. On the adsorption of proteins on solid surfaces, a common but very complicated phenomenon. J Biosci Bioeng 2001;9:233–44.
[46] Jefferson RA, Burgess SM, Hirsh D. β-Glucuronidase from *Escherichia coli* as a gene-fusion marker. Proc Natl Acad Sci U S A 1986;83:8447–51.
[47] Sakaguchi K, Matsui M, Mizukami F. Applications of zeolite inorganic composites in biotechnology: current state and perspectives. Appl Microbiol Biotechnol 2005;67:306–11.
[48] Sağ Y, Aktay Y. Mass transfer and equilibrium studies for the sorption of chromium ions onto chitin. Process Biochem 2000;36:157–73.
[49] Çelekli A, İlgün G, Bozkurt H. Sorption equilibrium, kinetic, thermodynamic, and desorption studies of Reactive Red 120 on *Chara contraria*. Chem Eng J 2012;191:228–35.
[50] Al-Ghouti M, Khraisheh MAM, Ahmad MNM, Allen S. Adsorption behaviour of methylene blue onto Jordanian diatomite: a kinetic study. J Hazard Mater 2009;165:589–97.
[51] Vadivelan V, Kumar KV. Equilibrium, kinetics, mechanism, and process design for the sorption of methylene blue onto rice husk. J Colloid Interface Sci 2005;286:90–100.
[52] Ho YS, Mckay G. Sorption of dyes and copper ions onto biosorbents. Process Biochem 2003;38:1047–61.
[53] Wang HL, Fei ZH, Chen JL, Zhang QX, Xu YH. Adsorption thermodynamics and kinetic investigation of aromatic amphoteric compounds onto different polymeric adsorbents. J Environ Sci 2007;19:1298–304.
[54] Liu Y. Is the free energy change of adsorption correctly calculated. J Chem Eng Data 2009;54:1981–5.
[55] Tu M, Pan X, Saddler JN. Adsorption of cellulase on cellulolytic enzyme lignin from lodgepole pine. J Agric Food Chem 2009;57:7771–8.
[56] Al-Ghouti M, Khraisheh MAM, Ahmad MNM, Allen S. Thermodynamic behaviour and the effect of temperature on the removal of dyes from aqueous solution using modified diatomite: a kinetic study. J Colloid Interface Sci 2005;28:6–13.